Deep Science Publishing, 2025
https://doi.org/10.70593/978-93-7185-269-2_6

Chapter 6: Wide-Tuning CMOS Reconfigurable Bandpass Filter for RF and Microwave Circuits

Aymen Ben Hammadi [1], Hatem Garrab [2,3], Sehmi Saad [4]

[1] *Dynamics RF/mmW consulting and design, RF and telecommunication department, 39 Street of Vercors, 38600, Grenoble, France.*
[2] *Electronics and Micro-Electronic Laboratory (LEμE), Bd de l'environnement, Monastir 5000, Tunisia.*
[3] *Higher Institute of Applied Sciences and Technology of Sousse, University of Sousse, Street Taher Ben Achour, 4003 Sousse, Tunisia.*
[4] *RF2S Spectrum Solutions, R&D department, 18 Street of the Faïencerie, 33300 Bordeaux, France.*

Abstract: The rapid development of modern wireless communication systems operating across multiple standards and frequency bands has intensified the need for reconfigurable RF and microwave front-end components. Among these, bandpass filters are essential for spectrum selectivity, interference suppression, and maintaining system linearity. This chapter provides a detailed overview of reconfigurable bandpass filter design in CMOS and hybrid technologies, emphasizing tuning techniques and integration challenges. It examines both passive and active approaches, including MEMS-based filters, acoustic-wave devices, piezoelectric LTCC implementations, and active topologies such as G_m-C, N-path, Q-enhanced LC, and active-inductor-based filters. Their tuning mechanisms, design trade-offs, and performance characteristics are thoroughly analyzed. The discussion highlights the advantages of active inductor-based designs in achieving compact size, wide tuning range, and high integration density while also addressing remaining challenges in noise and linearity for next-generation RF front-ends.

Keywords: RF and Microwave, Passive Bandpass Filter, Active Bandpass Filter, Tuning Range, Silicon Area, Power Consumption.

1 Introduction

The demand for high-performance, low-cost front-end modules has steadily increased since the last century, driven by advances in wireless communication technologies and the proliferation of standards. Within these systems, multi-frequency RF and microwave bandpass filters have become indispensable, enabling precise frequency selection and suppression of unwanted signals (Bhuiyan et al., 2018; Pactitis, 2018) while reducing overall system complexity (Christiano et al., 2003).

Substantial research has therefore focused on developing tunable BPF structures that maintain a constant quality factor during center-frequency adjustment (Joshi et al., 2009; Ghaffari et al., 2011; Wu et al., 2021). However, as noted by Jia et al. (2017) and Qin et al. (2017), many existing solutions require large silicon areas, making them unsuitable for compact implementations. Traditional passive BPFs, in particular, suffer from limitations such as poor compatibility with tuning elements, high insertion loss, and degraded electrical performance caused by technological constraints (Chaturvedi et al., 2017).

To overcome these drawbacks, active filter designs have gained prominence, offering better trade-offs between compactness, frequency tunability, quality factor, and integration. RF and microwave active BPFs have been successfully demonstrated in several technologies, enabling efficient RFIC implementations for high-frequency applications. Moreover, they support independent tuning of both center frequency and quality factor, aligning with the demands of modern communication systems. Despite these advantages, challenges persist in managing integration complexity, noise, linearity, and power consumption (Tow, 2009).

This chapter reviews the latest tunable technologies for RF and microwave circuits with a focus on bandpass filter design. It is structured as follows:

- Section 2 covers reconfigurable passive RF and microwave filters, including MEMS-based designs, SAW/BAW resonators, and LTCC filters.
- Section 3 discusses active filter approaches such as Gm-C, N-path, Q-enhanced LC, and active-inductor-based topologies.
- Section 4 provides a comparative analysis of these techniques, examining trade-offs in tuning range, integration density, linearity, and noise.
- Section 5 concludes by identifying promising research directions for next-generation reconfigurable RF front-ends.

2 Reconfigurable Passive RF and Microwave Filters

Passive filters play a key role in radio communication systems (Ma et al., 2023). Their extremely large dynamic range, often exceeding 100 dB, makes them indispensable for implementing filtering functions in transmission chains. This chapter reviews several passive filter topologies, focusing particularly on architectures that enable discrete tuning of reconfigurable parameters.

2.1 RF Filters Using MEMS Capacitors

Over the past decade, tunable RF bandpass filters using MEMS devices such as varactors and switched capacitors (Velagaleti et al., 2024; Jones et al., 2020) have been the subject of extensive research. These filters are attractive because they combine low insertion loss, high linearity, and strong power-handling capability with compact dimensions and good compatibility with microwave integrated circuits. However, most MEMS-based tunable RF filters face packaging-related reliability issues. In addition, their achievable shape factor and out-of-band rejection are often limited, as many reported designs employ low-order configurations, typically second-order coupled resonators.

An illustrative MEMS implementation is shown in Fig. 6.1, which presents the structure and photograph of a two-pole tunable filter. The design uses four identical tunable MEMS capacitors, labeled C_1, that provide center-frequency tuning and passband matching (Lin et al., 2018). These capacitors are paired with air-core inductors to form a High-Q LC tank circuit. For input and output matching, the design incorporates a shunt tunable capacitor (C_2) together with a fixed series capacitor (C_p) and an additional fixed capacitor (C_s).

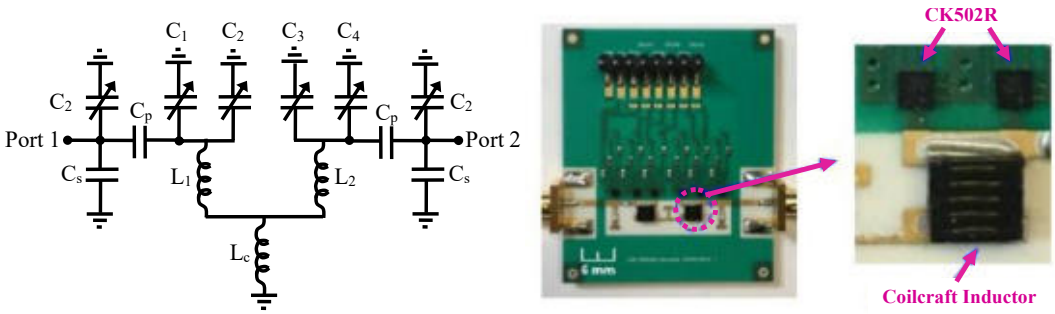

Fig. 6.1 (a) Two-pole tunable filter topology, and (b) the fabricated circuit.

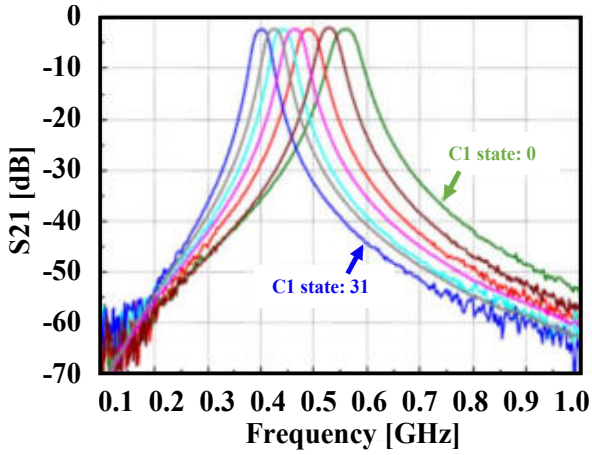

Fig. 6.2 Measured S_{21} response of the tunable filter.

The tuning range is achieved by varying the capacitance C_1 from 1 pF to 5 pF (see Fig. 6.2). Under these conditions, the measured input third-order intercept point (IIP3) lies between 35 dBm and 42 dBm, with a two-tone spacing of 5 MHz across the tuning band.

2.2 SAW and BAW RF Filters

Surface acoustic wave (SAW) and bulk acoustic wave (BAW) filters are electromechanical devices commonly used in the 100 MHz to 3 GHz range (Jang et al., 2021; Zhang et al., 2021; Seong et al., 2024). These devices are widely employed in satellite communications, radar receivers, and cellular systems.

Their operation is based on converting an electrical signal into an acoustic wave using an input transducer. The acoustic wave travels through a piezoelectric medium of length *l*, with a propagation velocity (υ) roughly five orders of magnitude slower than that of electromagnetic waves, allowing very compact structures. An output transducer then converts the acoustic wave back into an electrical signal. In BAW filters, acoustic waves propagate through the volume of thin piezoelectric layers, where mechanical and electrical energy are interchanged (Zhang et al., 2021).

A tunable bandpass filter based on RF SAW/BAW resonators was reported by (Komatsu et al. 2010). The ladder-type design, shown in Fig. 6.3, incorporates variable capacitors (VCs) both in series and parallel with the SAW/BAW resonators (Z_s and Z_p). The center frequency is tuned by adjusting the capacitances C_p and C_s.

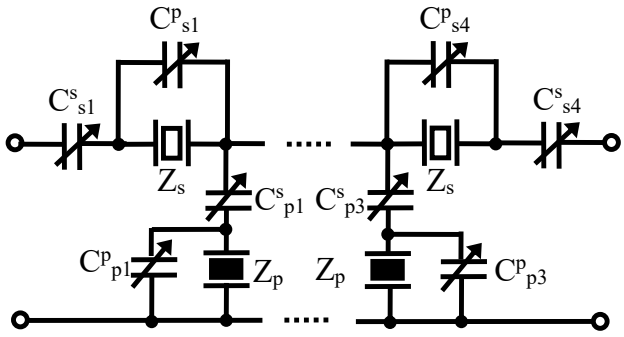

Fig. 6.3 SAW/BAW-based tunable filter configuration.

The circuit was fabricated on a Cu-grating/15-LN substrate as shown in Fig. 6.4(a). Measurement results shown in Fig. 6.4(b) indicate the center frequency of the filter can be tuned from 783 MHz to 913 MHz while the bandwidth remains approximately constant at 100 MHz.

2.3 Piezoelectric LTCC RF Filters

Piezoelectric LTCC filters are a subclass of the broader class known as dielectric filters. Piezoelectric low-temperature co-fired ceramic filters work on the basis of mechanical resonance of piezoelectric materials excited by electrical signals. The advantage of using ceramic-based materials, above all else, is the very low dielectric losses, high permittivity, and excellent thermal stability they exhibit (Sidorova et al., 2025). This allows for compact filters to have low insertion loss and high quality factors while making them well-suited for high-power RF applications.

A representative design of a tunable piezoelectric bandpass filter was reported in Ref. (Al-Ahmad et al., 2005). In this implementation, the key tuning element was a capacitor incorporating a high-permittivity dielectric layer with a piezo-electrically movable top electrode, illustrated in Fig. 6.5. A versatile mechanism for capacitance variation is implemented by this tunable varactor, achieved through controlled displacement of the electrodes.

The proposed varactor was integrated in a tunable piezoelectric filter that is shown in Fig. 6.6(a). The filter structure is based on two transmission-line sections. The first line, RF1, which has one end short-circuited to ground and the other terminated with the tunable capacitor, corresponds to the bottom metallization of the piezoelectric cantilever. The second line, RF2, is patterned on the LTCC substrate and serves as the fixed bottom electrode of the capacitor. Hence, the variable capacitor is defined by the overlapping area between RF1 and RF2, allowing the reconfiguration of the resonant frequency of the filter.

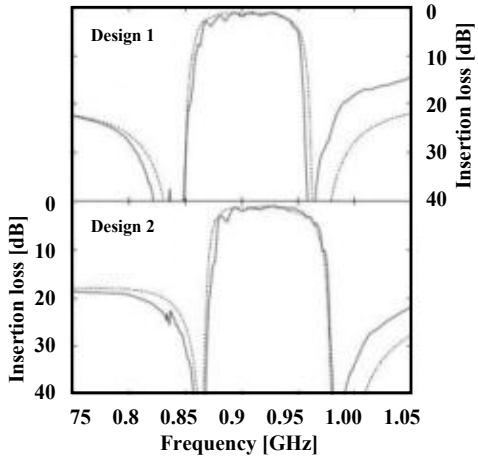

(a) (b)

Fig. 6.4 (a) Microscope image of a fabricated SAW/BAW filter, and (b) its frequency response.

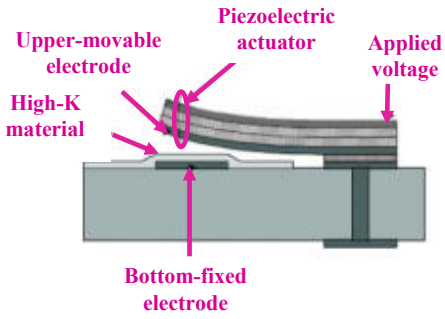

Fig. 6.5 Piezoelectric LTCC varactor schematic.

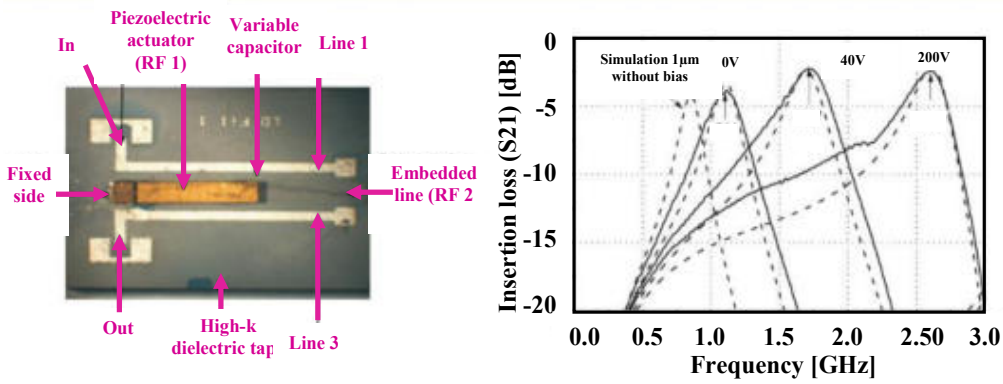

(a) (b)

Fig. 6.6 (a) Fabricated tunable bandpass filter, and (b) Its center frequency tuning with variable capacitor.

The measured frequency response of the proposed filter is shown in Fig. 6.6(b). A wide tuning range is obtained for a capacitance variation in which the center frequency can be tuned from 1.1 GHz to 2.6 GHz, representing 135% tuning range. Good input matching was also demonstrated, with return loss better than –11 dB within the tuning band, and a relatively low insertion loss over the entire operation range.

3 Reconfigurable Active RF and Microwave Filters

3.1 G_m-C RF Filters

Continuous-time G_m-C filters are a class of analog active filters, particularly well-suited to implement high-order filtering functions (>5) for high-frequency applications (Namdari et al., 2024; Oliveira et al., 2024). Their structure is based on the association

of a voltage-controlled transconductance element G_m with a capacitor C, as schematically depicted in Fig. 6.7.

The overall frequency response of the filter is set by the transfer function derived from this basic G_m–C building block, Equation 112:

$$\frac{V_{out}}{V_{in}} = \frac{G_m}{j\omega C} \tag{112}$$

The interest of G_m-C filters stems from the fact that their cut-off or center frequency is electronically tunable by means of the effective transconductance G_m. This is an attractive feature within the perspective of reconfigurable RF front-ends, which require adaptive frequency responses.

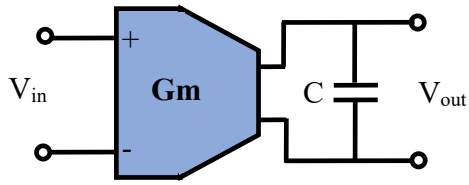

Fig. 6.7 Circuit schematic of a G_m-C filter, illustrating the basic topology using transconductors and capacitors.

A typical topology is illustrated in Fig. 6.8, representing a Chebyshev low-pass filter of order four, which was designed for channel selection in multi-mode wireless receivers (Abdulaziz et al., 2014). The circuit implements two cascaded sections of bi-quads to provide the second-order low-pass response. Fully-differential OTAs act as the active Gm cells, while MIM capacitors are used for the passive C elements in each stage of the bi-quads.

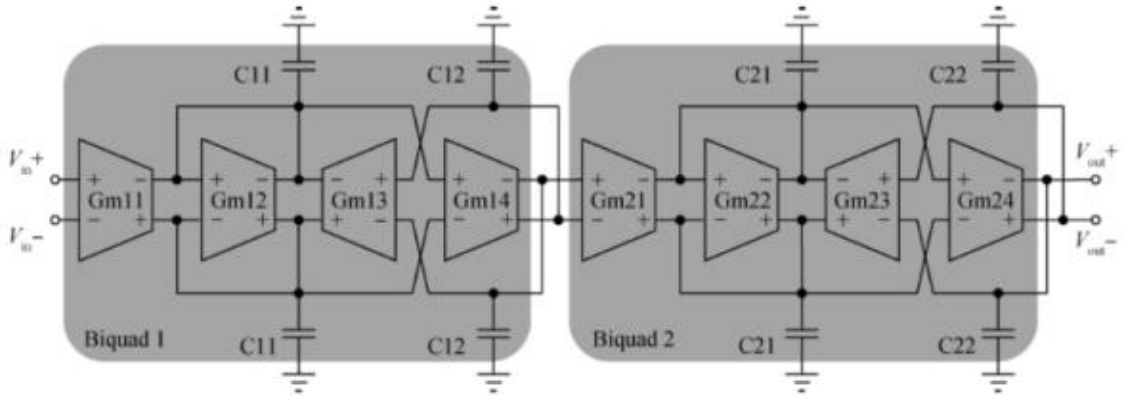

Fig. 6.8 Architecture of a fourth-order Chebyshev low-pass filter, showing cascade stages of bi-quads.

The measured frequency response of this implementation is shown in Fig. 6.9. The results show that the low-pass filter achieves a tunable cut-off frequency, from 322.5 kHz up to 20 MHz.

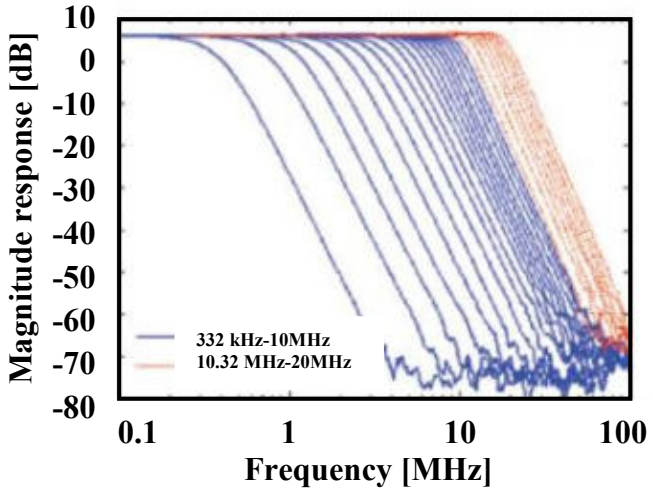

Fig. 6.9 Frequency response of the fourth-order Chebyshev low-pass filter.

Power consumption is directly proportional to the tuning condition, from a low of 4.2 mW for the lowest cutoff setting to a high of 9.5 mW for the highest under a supply voltage of just 1V. The suitability of G_m-C architectures to be integrated into reconfigurable RF systems is reinforced by such low-voltage, low-power operation.

3.2 N-Path RF Filters

N-path filters are a category of reconfigurable bandpass filters that leverage multiple parallel paths to accomplish frequency selectivity (Klumperink et al., 2022). From a conceptual standpoint, an N-path structure comprises N parallel channels, each including two mixers and a baseband transfer function block. The mixers effectively up-convert the baseband response into a bandpass response; hence, realizing a frequency-translated filtering function (Refer to Fig. 6.10). In the design methodology, lumped equivalents of quarter-wave transmission-line sections are usually used to implement series-LC-like N-path structures, which offer electrical isolation between adjacent filter paths and allow for the implementation of arbitrary selectivity higher-order filters.

Such a filter has been practically implemented in a 65 nm CMOS process, as shown in Fig. 6.11 (Reiskarimian et al., 2015). Measured performance metrics (Fig. 6.12a) show a tunable center frequency from 600 MHz to 850 MHz. Over this tuning range, the filter has an insertion loss between 4.7 dB and 6.2 dB for an adjustable bandwidth of 9–15 MHz, translating to a Q varying from 40 to 90.

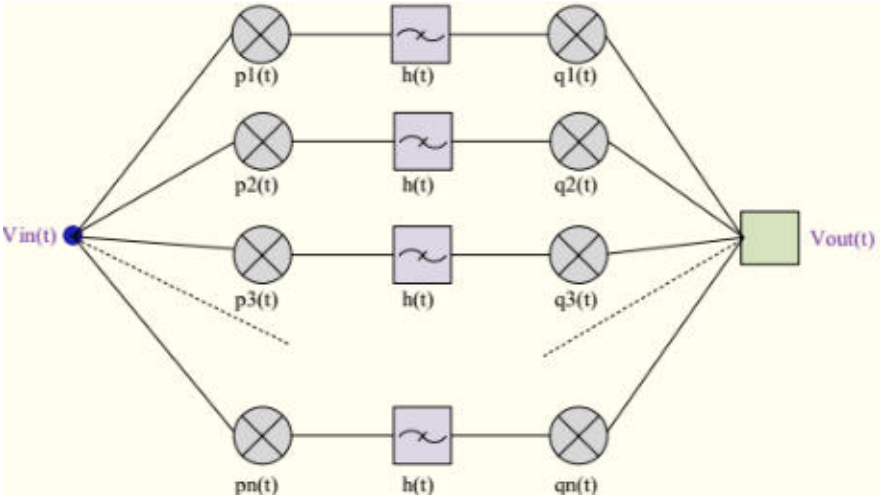

Fig. 6.10 Operating principle of the bandpass N-path filter.

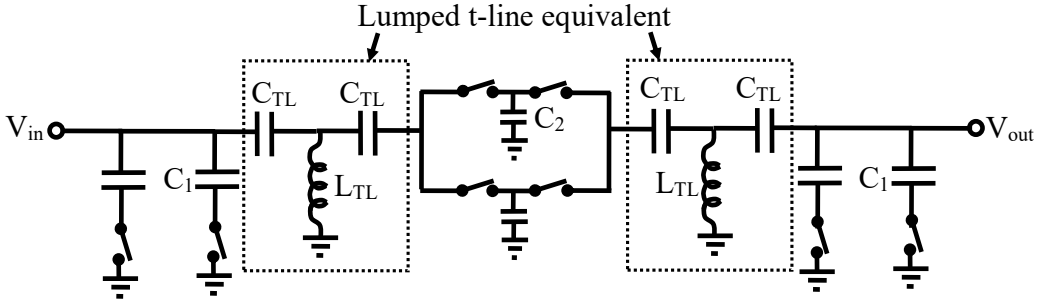

Fig. 6.11 Proposed architecture of an all-passive 6th-order (generally extendable to arbitrary order) N-path filter using CLC T-type quarter-wave transmission line equivalents.

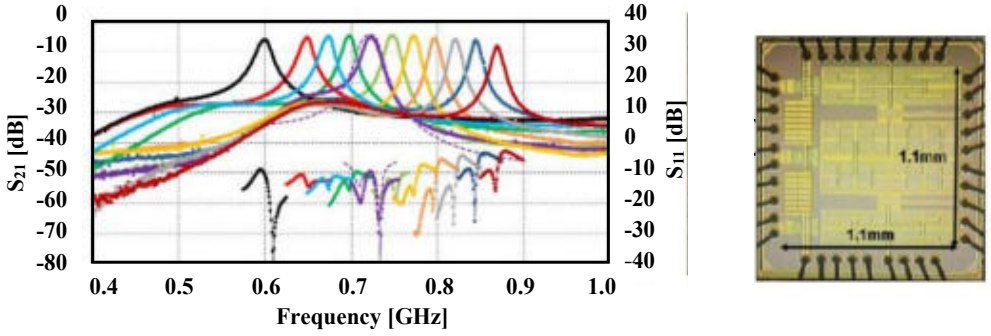

(a) (b)

Fig. 6.12 (a) Measured S_{21} (forward transmission) and S_{11} (input return loss) for various clock frequencies, demonstrating reconfigurability via CLC T-type networks, and (b) its photograph of the fabricated chip proposed by Reiskarimian et al. (2015).

Additional measured characteristics are a noise figure of approximately 8.5 dB, an input-referred 1 dB compression point (P1dB) of +7 dBm, and an input third-order intercept point (IIP3) of +17.5 dBm. The circuit operates from a 1.2 V supply voltage with a total power consumption of 75 mW.

These results evidence the potential of N-path filtering architectures for achieving reconfigurable bandpass responses within CMOS platforms, while making proper trade-offs among tunability, linearity, and noise performance.

3.3 LC (Q-Enhanced) RF Filters

LC filters, which can be implemented using integrated capacitors along with on-chip spiral inductors, are a popular solution for the integrated implementation of reconfigurable RF filters (Cortés et al., 2009). LC filters suffer from some problems: the low quality factor of the on-chip inductors, occupying a significant silicon area, and limited frequency tuning capability.

To overcome these shortcomings, a number of enhancement techniques have been suggested. Among the earliest and most popular methods, first proposed in the 1960s (Orchard et al., 1966) is the inclusion of an active device, which adds a negative resistance compensating for the intrinsic losses of the LC network. Filter topologies based on this approach are often called Q-enhanced filters because the quality factor of the resonator is enhanced by the additional active circuitry. A representative functional block diagram of a filter of that type is shown in Fig. 6.13.

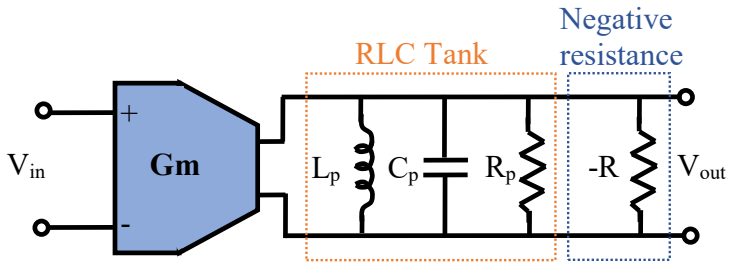

Fig. 6.13 Circuit structure of the LC filter with integrated compensation network.

The common architecture is an LC second-order bandpass filter with an input amplifier followed by an LC resonator (the so-called tank circuit). The tank circuit has a parasitic resistance R_p, which is mainly due to the inductor losses. These losses are compensated by adding a negative resistance circuit, the result of this approach being an increased sharpness of the resonance and thus a better selectivity. Another advantage of Q-enhanced LC filters is their ability to act as integrated solutions that replace rather bulky external filters like SAW, BAW, or ceramic filters, providing compact size, high

integration density, and performance at low supply voltages. Moreover, in contrast to G_m-C filters, LC-based Q-enhanced architectures can work effectively at frequencies up to the multi-GHz range, usually with lower power consumption (Loree et al., 2000).

A possible implementation of such a topology is shown in Fig. 6.14, representing a differential fourth-order filter structure with varactor diodes for frequency tuning (Amin et al., 2016). This method allows a higher range for tuning while preserving an elevated quality factor performance and, therefore Q-enhanced LC filters represent one of the attractive candidates for modern reconfigurable RF front-end systems.

The proposed filter contains an input voltage buffer that allows power-efficient gain control, which is especially needed when the quality factor (Q) of the BPF varies over a wide range. A variable transconductor is also added to the circuit in order to support current-mode operation and increase gain controllability. The outputs of the two signal paths are summed by subtraction utilizing an emitter follower pair (Q14-Q15) together with a common-emitter pair (Q16-Q17), resulting in a fourth-order BPF response.

The tunability of the filter quality factor is effected by two complementary control mechanisms. Firstly, Q is decreased by reducing the resistance R_c, which is a linear resistor in series with NMOS devices M1 and M2. Secondly, Q is increased by adding a negative resistance $-R_N$, which is provided by transistors Q5 through Q8 and resistors R_X and R_Y in Fig. 6.14.

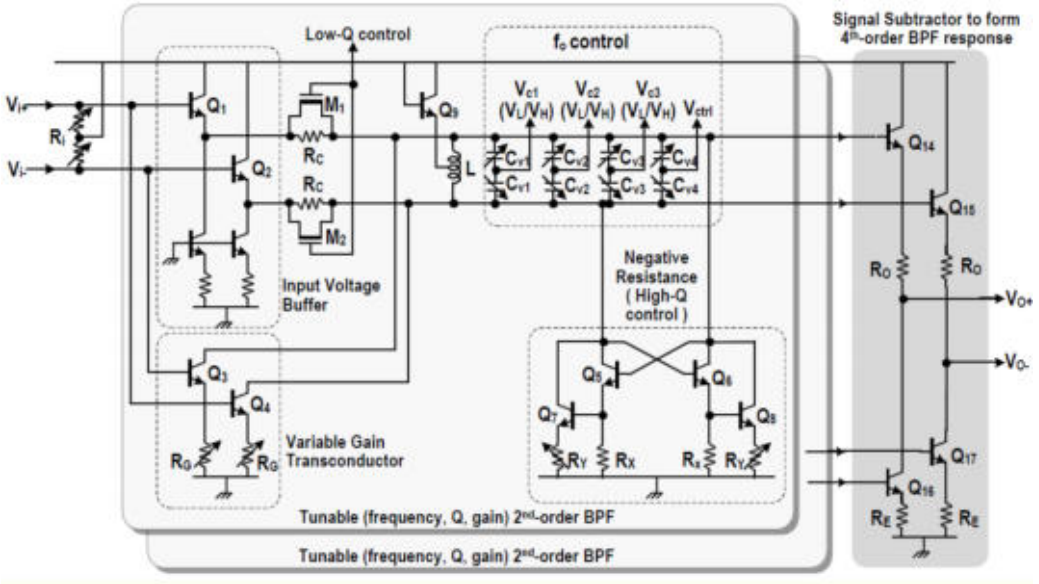

Fig. 6.14 Q-enhanced 4th-order differential BPF implementation.

The center frequency tuning is applied using a differential varactor bank C_{v1}-C_{v4}, combined with the integrated on-chip inductor L to form tunable LC tanks. Three

common tuning voltages V_{C1}-V_{C3} and two independent controls V_{ctrl1}, V_{ctrl2} set the varactors, allowing precise tuning into closely spaced frequency bands.

The circuit was fabricated in a 0.13 µm SiGe BiCMOS process and experimental verification of the prototype is presented. The measured frequency response for different states of tuning is displayed in Fig. 6.15(b). Based on the constant fractional bandwidth corresponding to Q≈20, a center frequency tuning range between 4.1 GHz and 7.9 GHz is achieved by changing the total varactor capacitance between 1.1 pF and 4.2 pF with a fixed inductor of 325 pH. Simultaneously, the insertion loss remains around 0 dB, while enabling tuning of the fractional bandwidth from 2% to 25%. In all, the measured noise figure is between 7.6 dB and 18 dB depending on the tuning state. The layout occupied a compact silicon area of 0.371 mm², while the power consumption was between 112 mW and 125 mW.

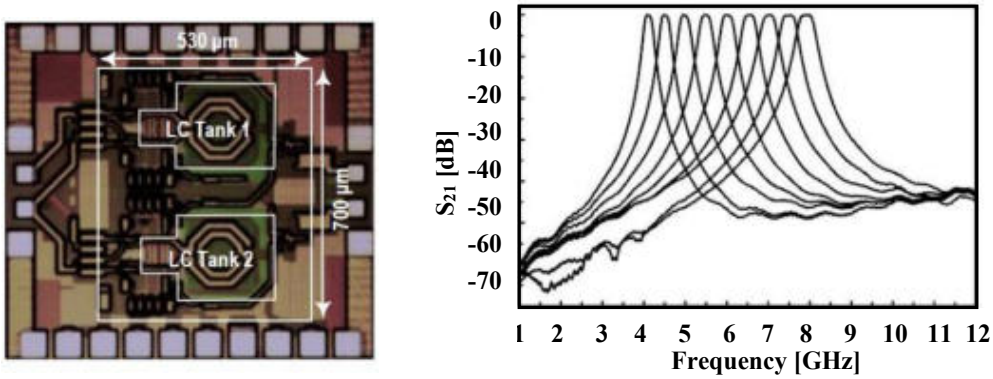

(a) (b)

Fig. 6.15 (a) The photograph of the fabricated tunable BPF, and (b) Its measured frequency tuning characteristics with constant fractional bandwidth.

3.4 RF Filters Using Active Inductor

During the last few years, TAI-based RF bandpass filters have become a critical block in modern state-of-the-art transceiver architectures. Unlike passive LC filters, these structures use only transistors, feedback loops, and negative resistance techniques to obtain a wide tunability range, high Q, and compact silicon footprint (Gorjizad et al., 2024; Saad et al., 2025).

Fig 6.17 depicts an example implementation of a second-order tunable BPF (Hammadi et al., 2017; Ben Hammadi et al., 2018). The filter follows three distinct stages in its architecture. The first stage is a fully differential input driver, comprising NMOS transistors M19 and M20; it converts the differential input voltage Vi_{n+} and V_{in-} into currents feeding the filter core. The second stage, containing the heart of the BPF,

employs two cascode-grounded active inductors that are coupled by means of a negative resistance to emulate not only an RLC tank but also to compensate for intrinsic losses so as to increase the Q-factor of the BPF. The third stage presents differential outputs V_{out+} and V_{out-} using NMOS source followers M21, M23, M22, M24, respectively; this helps the circuit drive on-chip 50 Ω loads efficiently over a wide RF range.

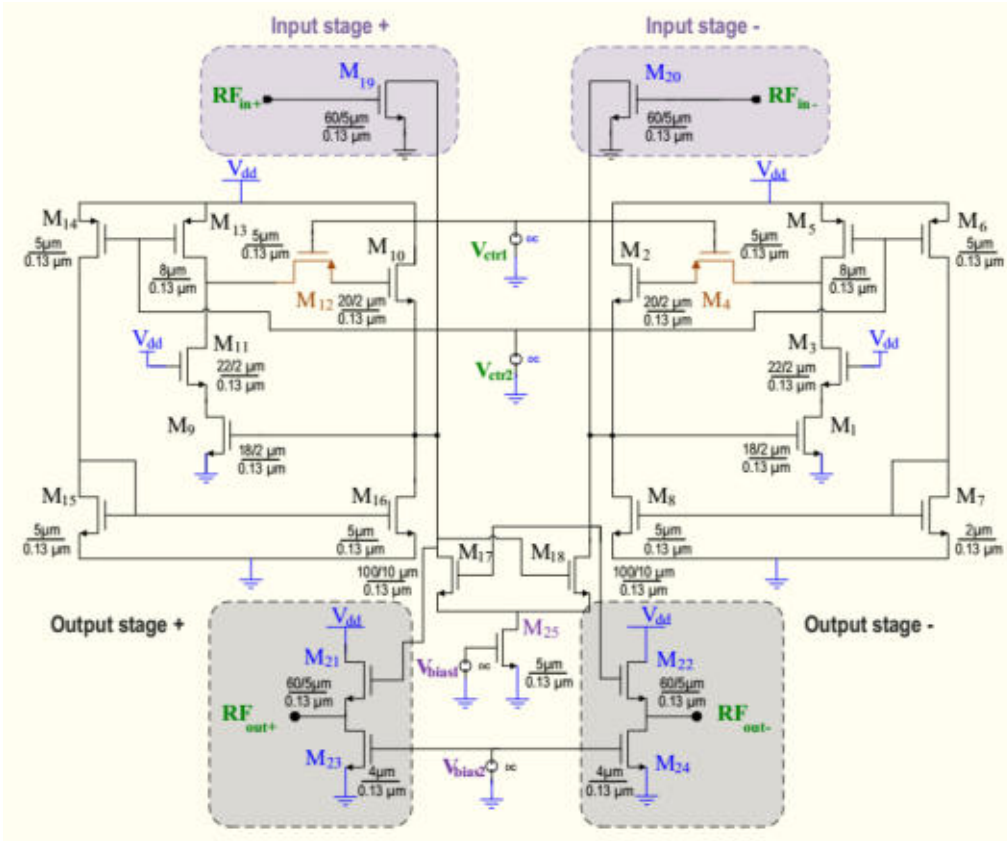

Fig. 6.17 Proposed reconfigurable bandpass filter.

The filter also supports multi-level tuning using biasing schemes:

- V_{ctr1} provides fine-tuning of the resonance frequency,
- V_{ctr2} controls the wideband frequency range,
- V_{bias1} controls the negative resistance magnitude, allowing Q to be adjusted.

Post-layout simulation results shown in Fig. 6.18 confirm the performance of the circuit. The center frequency can be tuned from 1.16 GHz to 3.27 GHz via control voltages, while the insertion loss is on average 30 dB, with a peak quality factor of 76.66 at 1.84 GHz. The filter effectively operates from 4.04 mA to 6.44 mA for the power consumption under a 1V supply.

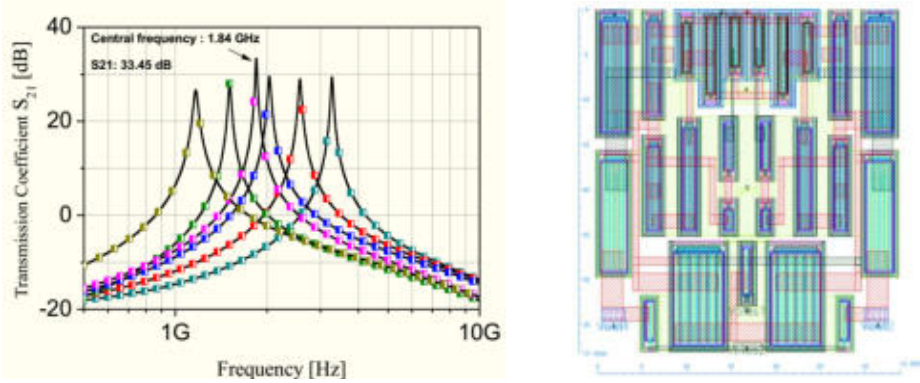

(a) (b)

Fig. 6.18 (a) Simulated S_{21} response of the active BPF vs. V_{ctr1} and V_{ctr2} (post-layout simulations), and (b) its lay-out.

4. Comparison

A range of tuning approaches has been described in the previous sections for RF and microwave filters that target a wide tuning range while achieving high performance. The filters were broadly divided into passive and active filters, further divided based on the underlying tuning technologies. Their key metrics are summarized in Table 6.1, providing a comparison of center frequency, tuning range, quality factor, insertion loss, power consumption, and integration density.

Based on this comparison, several important conclusions can be drawn:

- Active inductor-based structures offer the widest frequency tuning range, the highest quality factor, and the largest potential of integration in modern CMOS or BiCMOS processes.
- However, these benefits come with significant limitations. The most important are the noise performance and the linearity degradation that usually set the limit for their use in high dynamic-range applications.

Passive filter approaches like MEMS, SAW/BAW, or piezoelectric LTCC-based implementations usually provide superior noise characteristics and linearity; thus, they are well-suited for applications that demand high spectral purity. These are usually less flexible in terms of tuning and integration and normally require more area and additional packaging.

Table 6.1 Comparison of RF and microwave filter performances

Type	Technology	Tuning range	Center frequency	Quality factor (Q)	Insertion loss	Power consumption	Integration/Size	Noise
Passive filters	MEMS	Moderate	Low–Mid GHz	High	Low	None (passive)	Small, packaging required	Excellent
	SAW/BAW	Narrow	Low–Mid GHz	Moderate–High	Low	None (passive)	Very compact,	Excellent
	Piezoelectric	Wide	Mid GHz	High	Low	None (passive)	Small, stable	Good
Active filters	Gm–C	Wide	Low MHz	Moderate	Low	Low	Fully integrable	Sensitive
	N-Path (CMOS)	Moderate	Sub-GHz	Moderate–High	Moderate	High	On-chip CMOS	Moderate
	LC Q-enhanced	Wide	Multi-GHz	High (tunable)	Very low	High	Moderate area	Moderate
	Active inductor-	Wide	Multi-GHz	High	Variable	Low–Moderate	Very compact	Limited

Conclusion

Active RF filters using tunable inductors and Q-enhancement techniques have great potential for compact highly reconfigurable systems. In practice, however, their use must be carried out with careful consideration of the trade-offs between flexibility in tuning, integration density, and signal integrity metrics such as noise figure and linearity.

This chapter has provided an overview of recent wide-tunable passive and active filter designs. A variety of reconfigurable filter architectures have been presented: implementations based on passive tunable devices, MEMS, SAW/BAW technologies, and active solutions including piezoelectric, G_m-C, N-path, and Q-enhanced filters.

The comparative study of the various families developed for RF and microwave filters reveals that the most promising topology, which fits the targeted objectives, is the one based on active inductors. Indeed, the filters using active inductance exhibit outstanding advantages and perspectives for multiband communication systems: they combine compactness, wide tuning range, ease of integration, and low-cost tuning capability. Despite noise and linearity challenges, active inductor-based filters remain strong candidates for next-generation reconfigurable RF front-ends.

References

Abdulaziz, M., Törmänen, M., & Sjöland, H. (2014, September). A 4 th order Gm-C filter with 10MHz bandwidth and 39dBm IIP3 in 65nm CMOS. In ESSCIRC 2014-40th European Solid State Circuits Conference (ESSCIRC) (pp. 367-370). IEEE.

Al-Ahmad, M., Maenner, R., Matz, R., & Russer, P. (2005, June). Wide piezoelectric tuning of LTCC bandpass filters. In IEEE MTT-S International Microwave Symposium Digest, 2005. (pp. 1275-1278). IEEE.

Amin, F., Raman, S., & Koh, K. J. (2016, May). A high dynamic range 4th-order 4–8 GHz Q-enhanced LC band-pass filter with 2–25% tunable fractional bandwidth. In 2016 IEEE MTT-S International Microwave Symposium (IMS) (pp. 1-4). IEEE.

Ben Hammadi, A., Haddad, F., Mhiri, M., Saad, S., & Besbes, K. (2018). RF and microwave reconfigurable bandpass filter design using optimized active inductor circuit. International Journal of RF and Microwave Computer-Aided Engineering, 28(9), e21550.

Bhuiyan, M. A., Reaz, M. B. I., Omar, M. B., Badal, M. T. I., & Jahan, N. A. (2018). Advances in active inductor based CMOS band-pass filter. Micro and Nanosystems, 10(1), 3-10.

Chaturvedi, S., Božanić, M., & Sinha, S. (2017, April). A 50 GHz SiGe BiCMOS active bandpass filter. In 2017 IEEE 20th International Symposium on Design and Diagnostics of Electronic Circuits & Systems (DDECS) (pp. 2-5). IEEE.

Christiano, L. J., & Fitzgerald, T. J. (2003). The band pass filter. International economic review, 44(2), 435-465.

Cortés, P., Ortiz, G., Yuz, J. I., Rodríguez, J., Vazquez, S., & Franquelo, L. G. (2009). Model predictive control of an inverter with output $ LC $ filter for UPS applications. IEEE Transactions on industrial electronics, 56(6), 1875-1883.

Gorjizad, Z., Shojaee, A., & Abrishamifar, A. (2024). A compact and tunable active inductor-based bandpass filter with high quality factor for Wireless LAN applications. AEU-International Journal of Electronics and Communications, 187, 155540.

Jang, Y., Kim, J., Ha, J., Kim, D., Lim, J., Han, S. M., & Ahn, D. (2021, November). A design method of wideband BPF considering frequency dependence of inverters for SAW filter. In 2021 IEEE MTT-S International Microwave Filter Workshop (IMFW) (pp. 185-188). IEEE.

Jia, D. H., & Deng, J. (2017, November). Tunable microstrip bandpass filter based on cascade quadruplet topology. In 2017 Progress in Electromagnetics Research Symposium-Fall (PIERS-FALL) (pp. 777-779). IEEE.

Jones, T. R., & Daneshmand, M. (2020). Miniaturized folded ridged quarter-mode substrate integrated waveguide RF MEMS tunable bandpass filter. IEEE Access, 8, 115837-115847.

Joshi, H., Sigmarsson, H. H., Moon, S., Peroulis, D., & Chappell, W. J. (2009). High-$ Q $ fully reconfigurable tunable bandpass filters. IEEE transactions on microwave theory and techniques, 57(12), 3525-3533.

Klumperink, E., & Nauta, B. (2022). N-path filters and mixer-first receivers–a review. IC Design Insights-from Selected Presentations at CICC 2017, 221-264.

Komatsu, T., Hashimoto, K. Y., Omori, T., & Yamaguchi, M. (2010). Tunable radio-frequency filters using acoustic wave resonators and variable capacitors. Japanese Journal of Applied Physics, 49(7S), 07HD24.

Lin, T. W., Gao, L., Gaddi, R., & Rebciz, G. M. (2018). 400–560 MHz tunable 2-pole RF MEMS bandpass filter with improved stopband rejection 2018 IEEE/MTT-S Int. Microwave Symp. IMS.

Loree, D. L., & O'Loughlin, J. P. (2000, June). Design optimization of LC filters. In Conference Record of the 2000 Twenty-Fourth International Power Modulator Symposium (pp. 137-140). IEEE.

Ma, H., Hu, Z., & Yu, D. (2023). A low-loss bandpass filter with stacked double-layer structure using glass-based integrated passive device technology. IEEE Electron Device Letters, 44(7), 1216-1219.

Namdari, A., Aiello, O., & Caviglia, D. D. (2024). A 0.5 V, 32 nW Compact Inverter-Based All-Filtering Response Modes Gm-C Filter for Bio-Signal Processing. Journal of Low Power Electronics and Applications, 14(3), 40.

Oliveira, M. S., Carvalho, M. B., Müller, C., Compassi-Severo, L., de Aguirre, P. C., & Girardi, A. G. (2024). Design and Characterization of a Digitally Tunable Gm-C Filter for Multi-Standard Receivers. Electronics, 13(14), 2866.

Orchard, H. J. (1966). Inductorless filters. Electronics letters, 2(6), 224-225.

Pactitis, S. A. (2018). Active filters: theory and design. CRC press.

Qin, W., Cai, J., Li, Y. L., & Chen, J. X. (2017). Wideband tunable bandpass filter using optimized varactor-loaded SIRs. IEEE Microwave and Wireless Components Letters, 27(9), 812-814.

Reiskarimian, N., & Krishnaswamy, H. (2015, May). Design of all-passive higher-order CMOS N-path filters. In 2015 IEEE Radio Frequency Integrated Circuits Symposium (RFIC) (pp. 83-86). IEEE.

Saad, S., Haddad, F., & Ben Hammadi, A. (2025). A Compact and Tunable Active Inductor-Based Bandpass Filter with High Dynamic Range for UHF Band Applications. Sensors, 25(10), 3089.

Seong, M., Kim, J., & Eo, Y. (2024). SAW device with reactive reflector for integrated SAW RF duplexer area minimization. IEEE Transactions on Electron Devices.

Sidorova, S. V., & Khokhlun, S. A. (2025, April). The Properties Investigation Results of Low-Temperature Co-Fired Ceramics. In 2025 7th International Youth Conference on Radio Electronics, Electrical and Power Engineering (REEPE) (pp. 1-6). IEEE.

Tow, J. (2009). A step-by-step active-filter design. IEEE Spectrum, 6(12), 64-68.

Velagaleti, S. B., & Siddaiah, N. (2024). Analysis of A Semi-Circular Cavity BPF with RF-MEMS Switches for 5G Applications and X-band Satellite Communication applications.

Wu, Y., Fourn, E., Besnier, P., & Quendo, C. (2021). Direct synthesis of multiband bandpass filters with generalized frequency transformation methods. IEEE Transactions on Microwave Theory and Techniques, 69(8), 3820-3831.

Zhang, L., Yu, H., Jiang, M., Deng, L., Zhou, X., Wang, X., ... & Jiang, C. (2021, May). A 6–18 GHz Multifunction Heterodyne RF Transceiver Module on LTCC with SAW and BAW Bandpass Filters. In 2021 IEEE MTT-S International Wireless Symposium (IWS) (pp. 1-3). IEEE.